

## EXCITATION FUNCTIONS OF (p,xn) REACTIONS ON NATURAL TELLURIUM AT LOW ENERGY CYCLOTRON: RELEVANCE TO THE PRODUCTION OF MEDICAL RADIOISOTOPE $^{123}\text{I}$

K. Zarie<sup>1</sup>, N. A. Hammad<sup>1</sup>, A. Azzam<sup>2</sup>

<sup>1</sup>Physics Department, Girls College of Education in Riyadh, Scientific  
Departments, Saudi Arabia.

<sup>2</sup>Nuclear Physics Department, Nuclear Research Center, Atomic Energy  
Authority, Cairo, Egypt.

E-mail: n\_al\_hammad@hotmail.com

Rec. 16/ /2006

Accept. 24/5/2006

Excitation functions of the nuclear reactions  $^{nat}\text{Te}(p,xn)^{121,123,124,126,128,130}\text{I}$  were measured, using the stacked foil technique for proton energies starting from the respective reaction thresholds up to 27.5 MeV. Thin uniform films of  $^{nat}\text{Te}$  on Ti-backing were prepared by the electrodeposition method. At energies less than 20 MeV the present data agree within the experimental errors with the literature values. Above 20 MeV new experimental cross section values have been recorded. The Integral yield of  $^{123}\text{I}$  with its radionuclidic impurity  $^{121,124,126,128,130}\text{I}$  were calculated from the measured cross section data.

**Keywords:** Excitation function, proton reactions,  $^{nat}\text{Te}$   $^{123}\text{I}$ , integral yields, radionuclide impurity.

### INTRODUCTION

The radioisotope  $^{123}\text{I}$  ( $T_{1/2}=13.2$  h; EC = 100%;  $E_{\gamma}=159$  keV;  $I_{\gamma}=83.3\%$ ) is an ideal radionuclide for in-vivo medical diagnostic studies using Single Photon Emission Tomography (SPECT). For the production of  $^{123}\text{I}$  about 25 nuclear reactions have been investigated [1]. Among them only four are of significance. At low energy cyclotrons the  $^{123}\text{Te}(p,n)$  reaction over  $E_p = 14.5 - 10$  MeV is the predominating one [2,3]. At a medium energy cyclotrons the  $^{124}\text{Te}(p,2n)$  reaction over  $E_p = 26 - 23$  MeV is the leading route [2,3]. In either cases highly enriched target material is used. The recovery

of  $^{123}\text{I}$  is rather easy. The irradiated  $^{123}\text{TeO}_2$  or  $^{124}\text{TeO}_2$  target is heated at  $755\text{ }^\circ\text{C}$  (just above the m.p. of  $\text{TeO}_2$ ) in a stream of oxygen whereby radioiodine is removed and taken up in a small amount of water. The target is regenerated and is ready for reuse [4].

The third route of  $^{123}\text{I}$ - production is the  $^{127}\text{I}(p,5n)^{123}\text{Xe} \xrightarrow{\text{EC}\beta\ 72.1\text{ h}} ^{123}\text{I}$  reaction. The optimum energy range for this reaction is  $E_p = 65 - 45\text{ MeV}$ . Thus it needs a higher energy cyclotron. The removal of radioxenon from the irradiated NaI target is done either on-line, i.e. during the irradiation in a flow system, or off-line, i.e. after the end of the irradiation in a batch mode. The collected radioxenon is allowed to decay for about 7 h during which period the maximum growth of  $^{123}\text{I}$  occurs. Thereafter  $^{123}\text{I}$  is removed from the vessel containing radioxenon [2,3].

The fourth route of  $^{123}\text{I}$ - production is the  $^{124}\text{Xe}(p,x)$  reaction. It involves highly enriched  $^{124}\text{Xe}$  but requires only a medium-sized cyclotron. The development of this reaction clearly demonstrates the changing demands on the quality of the medically important radionuclides. In contrast to the above mentioned three routes, this reaction leads to  $^{123}\text{I}$  of the highest purity. The natural abundance of  $^{124}\text{Xe}$  is only 0.1% ; consequently the highly enriched  $^{124}\text{Xe}$  is very expensive [5].

The radioisotope  $^{124}\text{I}$  ( $T_{1/2}=4.18\text{ d}$ ;  $E_{\beta^+}=2.13\text{ MeV}$ ;  $I_{\beta^+}=25\%$ ) is the only longer-lived  $\beta^+$  emitting radioisotope of iodine and has found application in labelling biomolecules, especially in tumour research [6,7]. It is suitable for both diagnostic with Positron Emission Tomography (PET) and therapeutic use in nuclear medicine [8].

## EXPERIMENTAL

The excitation functions were measured by the stacked foil technique used to the first time at (CS30) cyclotron at King Faisal Specialized Hospital and Research Center (KFSH&RC) during this work. Some pertinent details relevant to the present work are given below.

### Preparation of Thin Target Samples

High purity natural tellurium (>99.9% supplied by Goodfellow Metals, England) was used as target material. Its natural isotopic abundance (in %) was:  $^{108}\text{Te}$  (0.096),  $^{122}\text{Te}$  (2.603),  $^{123}\text{Te}$  (0.903),  $^{124}\text{Te}$  (4.186),  $^{125}\text{Te}$  (7.139),  $^{126}\text{Te}$  (18.95),  $^{128}\text{Te}$  (31.69) and  $^{130}\text{Te}$  (33.80). Thin target samples were prepared by electrodepositing Te onto 12  $\mu\text{m}$  thick Ti foils (>99.9% pure) supplied by Goodfellow Metals, England) of 8 mm diameter. The electrolytic mixture used contained 1 g of  $\text{TeO}_2$  and 2.5 g of KOH dissolved all in 50 ml D.I. water. Only foils with a homogeneous black deposit were used and the following conditions were found suitable: voltage 2–2.6V, current intensity 10–15 mA, electro plating time 20–26 min. After drying and weighing, the

thick of the deposited tellurium layer was (between 15 and 20  $\mu\text{m}$ ). The deposited target was covered by 50  $\mu\text{m}$  thick pure Al foil (>99.9%) supplied by Goodfellow Metals, England) to protect them and to avoid any loss of tellurium or radioiodine. The sandwich sample (Ti—Te—Al) was then ready for irradiation.

### Irradiation and Beam Current Monitoring

Two stacks (a total of 38 sandwich samples and several 10  $\mu\text{m}$  thick Cu foils serve as energy degrader and monitor foils) were irradiated with proton beam current of about 100 nA for 30 min in the external beam channel of (CS30) cyclotron at (KFSH&RC). The stacks were irradiated in a Faraday cup with a secondary electron suppressor, which served also as target holder. The collected charges were integrated using current integrator circuit. An earthed 8 mm diameter collimator was placed in front of the target. The beam current was kept constant throughout each irradiation. The energy degradation along the stacks was determined by using a computer code based on well-measured stopping power data [9].

The beam current was monitored up to 27.5 MeV via the  $^{nat}\text{Cu}(p,x)^{62}\text{Zn}$ ,  $^{nat}\text{Cu}(p,x)^{63}\text{Zn}$  and  $^{nat}\text{Cu}(p,x)^{65}\text{Zn}$  reactions. The excitation functions of these monitor reactions were compared to the recommended data reported by the International Atomic Energy Agency [IAEA TECDOC-1211, 2001] [10], which shows an acceptable agreement with our data. For a further check the reaction  $^{nat}\text{Ti}(p,x)^{48}\text{V}$  induced in the Ti-backing foils was also used as monitor, and there was also a good agreement with the recommended data of the IAEA [10].

### Measurement of Radioactivity

The radioactivity of each irradiated sample and monitor foil was determined non-destructively by  $\gamma$ -ray spectrometry using a HpGe detector after about 30 min from the end of the irradiations without removing the Al cover-foil. The detector absolute efficiency was about 42% while its resolution was 1.9 keV at the 1.33 MeV  $\gamma$ -line of  $^{60}\text{Co}$ . The detector source distance was kept long enough to keep the dead time of the system less than 8%, to assure point source like geometry and minimal pile up losses. Special attention was paid to the efficiency calibration of the detector over the whole required energy range, using several standard point  $\gamma$ -sources of known activity. To minimize the relative errors of the calibration curve, several gamma lines were used in order to determine the activity for a given radionuclide, where it was possible. The decay parameters for the mentioned isotopes and monitor products, given in Table 1, were taken from Firestone [1].

The Q-values of the energetically possible contributing reactions of the iodine isotopes were calculated, using ref. [12], and presented in Table 2. The contribution of the  $^{47}\text{Sc}$ , formed from the  $^{nat}\text{Ti}(p,x)^{47}\text{Sc}$ , to the  $\gamma$ -line of 159 keV, which was used for activity determination of  $^{123}\text{I}$ , was subtracted.

**Table 1.** Decay data for the investigated radionuclides.

Nuclide	Half life	$E_{\gamma}$ (keV)	$I_{\gamma}$ (%)	Mode of decay (%)
<b>Reaction Products</b>				
$^{121}\text{I}$	2.12 h	212.19	84	EC (100)
$^{123}\text{I}$	13.27 h	158.97	83	EC (100)
$^{124}\text{I}$	4.17 d	602.73	63	$\beta^+$ (25)
		1690.98	10.88	EC (75)
		722.7	10.35	
$^{126}\text{I}$	13.11 d	666.33	33.1	$\beta^+$ (43.7)
		753.81	4.16	EC (56.3)
$^{128}\text{I}$	24.99 m	442.22	17	$\beta^-$ (93.1), EC (6.9)
$^{10}\text{I}$	12.36 h	536.09	99	$\beta^-$ (100)
		668.54	96	
		739.48	82	
<b>Monitor Products</b>				
$^{48}\text{V}$	15.97 d	983.52	99.98	$\beta^+$ (49.6)
		1312.09	97.5	EC (50.4)
		944.1	7.76	
$^{62}\text{Zn}$	9.26 h	596.7	25.7	$\beta^+$ (6.9)
		548.4	15.2	EC (93.1)
$^{63}\text{Zn}$	38.4 m	669.8	8.5	$\beta^+$ (93), EC (7)
$^{65}\text{Zn}$	224.26d	1115.5	50.6	$\beta^+$ (1.5), EC (98.5)

**Table 2.** Contributing reactions for the investigated radioiodines.

Nuclide	Contributing reactions	Q-value (MeV)	E <sub>thr</sub> (MeV)
<sup>121</sup> I	<sup>122</sup> Te(p,2n) <sup>121</sup> I	-12.87689	12.98335
	<sup>123</sup> Te(p,3n) <sup>121</sup> I	-19.80637	19.96879
<sup>123</sup> I	<sup>123</sup> Te(p,n) <sup>123</sup> I	-2.01659	2.03313
	<sup>124</sup> Te(p,2n) <sup>123</sup> I	-11.44189	11.53496
	<sup>125</sup> Te(p,3n) <sup>123</sup> I	-18.018	18.16338
	<sup>126</sup> Te(p,4n) <sup>123</sup> I	-27.1319	27.34908
<sup>124</sup> I	<sup>124</sup> Te(p,n) <sup>124</sup> I	-3.94196	3.97403
	<sup>125</sup> Te(p,2n) <sup>124</sup> I	-10.51807	10.60293
	<sup>126</sup> Te(p,3n) <sup>124</sup> I	-19.63197	19.78911
<sup>126</sup> I	<sup>126</sup> Te(p,n) <sup>126</sup> I	-2.93771	2.96123
	<sup>128</sup> Te(p,3n) <sup>126</sup> I	-18.00381	18.14568
<sup>128</sup> I	<sup>128</sup> Te(p,n) <sup>128</sup> I	-2.03417	2.0502
	<sup>130</sup> Te(p,3n) <sup>128</sup> I	-16.53623	16.66452
<sup>130</sup> I	<sup>130</sup> Te(p,n) <sup>130</sup> I	-1.20271	1.21204

### Calculation of Cross-Sections and Errors

From the measured decay rates of the radioactive products and the measured beam currents, the cross-sections were calculated using the usual activation formula. The total error in the measured cross-section (10-15%) was obtained by combining uncertainty on each measured cross section value, by taking the positive square root of the summation of the following contributing sources: uncertainty on number of target atoms (5%), nuclear data (5%), beam intensity (7%), absolute efficiency of the spectrometer (3—7%), statistical and peak fitting uncertainty (1—10%), in quadrature supposing equal sensitivity coefficients.

## RESULTS AND DISCUSSION

### Excitation Functions

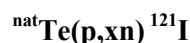
The numerical values of the measured cross sections together with the estimated errors for the (p, xn) reactions on  $^{nat}\text{Te}$  leading to the formation of  $^{121,123,124,126,128,130}\text{I}$  are given in Table 3.

**Table 3.** Measured cross sections of proton induced reactions on  $^{nat}\text{Te}$ .

Energy (MeV)	Cross section (mbarn) for production of :					
	$^{121}\text{I}$	$^{123}\text{I}$	$^{124}\text{I}$	$^{126}\text{I}$	$^{128}\text{I}$	$^{130}\text{I}$
4.812		0.04±0.01	0.44±0.07	1.37±0.21		0.98±0.15
7.335	0.93±0.14	0.93±0.14	1.59±0.24	9.26±1.39		4.65±0.70
8.355		1.41±0.21	0.92±0.14	24.03±3.60		10.19±1.53
9.267		1.91±0.29	3.34±0.50	56.04±8.41		50.75±7.61
9.711					49.32±7.39	
10.111	1.27±0.19	2.18±0.33	9.27±1.39	70.95±10.64		93.37±14.01
10.588					73.97±11.09	
11.006	1.65±0.25	5.26±0.79	18.54±2.78	89.80±13.47		95.83±14.38
11.414					85.74±12.86	
12.805	2.12±0.32	12.14±1.82	32.88±4.93	83.23±12.49		89.10±13.37
13.56					52.99±7.99	
13.569	3.28±0.49	19.81±2.97	59.78±8.97	78.88±11.83	53.25±7.99	80.01±12.00
14.283	4.16±0.62	35.30±5.30	74.63±11.19	55.42±8.31		74.54±11.18
14.965	4.62±0.69	38.50±5.78	76.97±11.55	30.56±4.58		71.33±10.70
15.588	6.08±0.91	42.20±6.33	84.57±12.69	21.24±3.19		68.38±10.26
15.786					39.50±5.92	
16.046					34.69±5.20	
16.188	8.44±1.27	47.45±7.12	82.03±12.30	16.91±2.55		69.41±10.41
16.787	11.47±1.72	48.88±7.66	87.91±13.19	13.23±1.98		68.93±10.33
17.362	15.93±2.39	51.87±7.78	88.70±13.31	11.51±1.73		68.22±10.23
17.925	16.87±2.53	54.45±8.17	90.22±13.53	9.38±1.41		70.09±10.51
18.472	17.86±2.68	51.19±7.53	89.89±13.48	5.93±0.89	17.84±2.67	68.08±10.21
19.013	20.99±3.15	51.88±7.68	81.56±12.23	7.39±1.12		67.99±10.19
19.543	19.18±2.88	55.16±8.27	79.40±11.91	7.46±1.12	13.89±2.08	69.33±10.40
20.062	27.97±4.20	60.04±9.01	82.56±12.38	9.71±1.46	3.04±0.46	69.73±10.46
20.566	31.84±4.78	67.29±10.09	85.83±12.87	8.34±1.25	0.86±0.13	69.08±10.36
21.062	65.86±9.88	81.87±12.28	87.83±13.17	13.87±2.08	1.47±0.22	67.07±10.06
21.551	98.12±14.72	96.79±14.52	89.41±13.41	18.26±2.74	2.17±0.35	69.17±10.38
22.026	105.94±15.89	109.68±16.45	91.67±13.75	22.86±3.43	2.05±0.31	68.48±10.27
22.506	141.94±21.29	125.65±18.85	93.84±14.08	28.44±4.23	3.15±0.47	67.26±10.09
22.984	184.44±27.67	131.29±19.69	92.52±13.88	35.39±5.31	3.07±0.46	68.15±10.22

**Table3. Continued**

Energy (MeV)	Cross section (mbarn) for production of :					
	$^{121}\text{I}$	$^{123}\text{I}$	$^{124}\text{I}$	$^{126}\text{I}$	$^{128}\text{I}$	$^{130}\text{I}$
23.441	268.30±40.25	138.32±20.75	92.69±13.90	38.99±5.84	3.66±0.55	68.64±10.30
23.886	307.11±46.07	140.78±21.12	90.06±13.51	40.78±6.12	4.07±0.61	66.43±9.96
24.325	329.59±49.44	149.45±22.42	93.25±13.99	41.30±6.19	4.46±0.67	68.33±10.25
24.757	358.08±53.71	155.33±23.30	93.50±14.03	43.64±6.55	4.13±0.62	68.46±10.27
25.183	361.67±54.25	152.64±22.89	90.99±13.65	49.98±7.50	4.47±0.67	65.98±9.90
25.609	365.04±54.76	154.89±23.23	94.9±14.24	53.87±8.08	4.52±0.68	68.32±10.25
26.028	367.90±55.18	159.74±23.96	93.91±14.08	52.44±7.87	4.52±0.68	66.37±9.96
26.448	361.98±54.3	156.92±23.54	95.12±14.27	54.19±8.13	4.73±0.71	69.81±10.47
26.855	360.47±54.07	159.72±23.96	96.88±14.53	59.61±8.94	4.62±0.69	64.56±9.68



The cross section values of the present work are presented with the available reported results in Figure 1. Small contribution of the  ${}^{122}\text{Te}(\text{p},2\text{n}) {}^{121}\text{I}$  reaction to the cross-section value, with a maximum value of about 20 mb, can be seen at  $E_p \leq 19$  MeV. The contribution of  ${}^{123}\text{Te}(\text{p},3\text{n}) {}^{121}\text{I}$  reaction starts at 19.9 MeV and reaches a

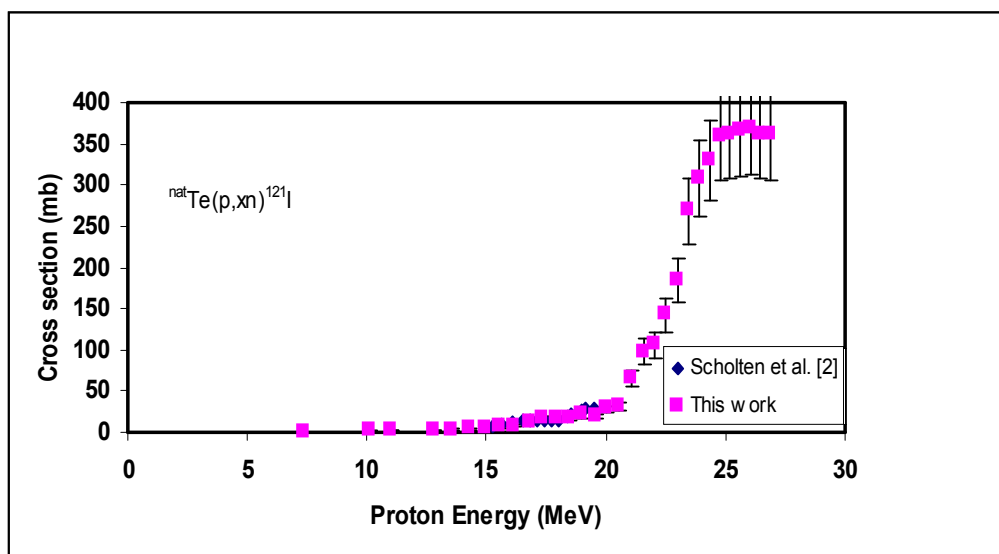


**Figure 1.** Excitation function of  ${}^{\text{nat}}\text{Te}(\text{p},\text{xn}) {}^{121}\text{I}$  reaction along with the previously available experimental data[2].

maximum value of 367.9 mb at about 26 MeV. The present cross-section data are in good agreement with the only reported cross-section values, Scholten et al. [2] in the

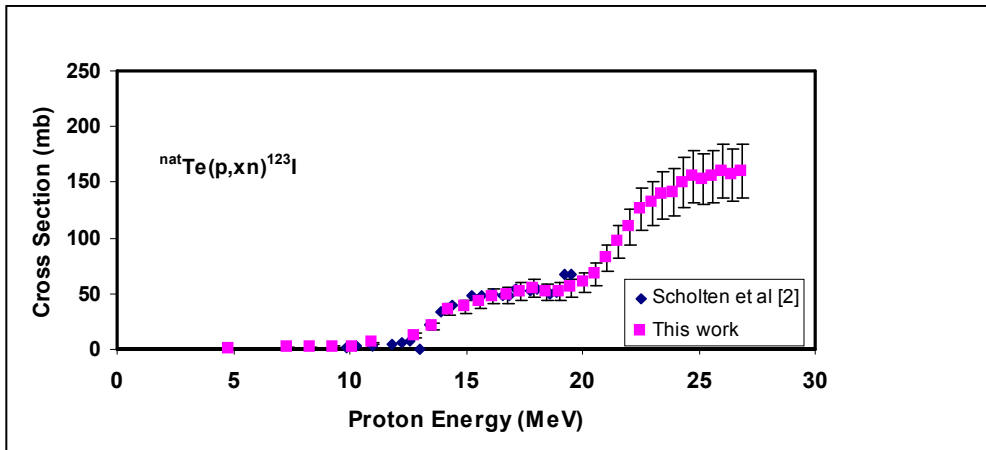
limited reported energy range ( $E_p \leq 18$  MeV). Due to, the lack of full information on irradiation conditions on  $^{nat}\text{Te}(p,xn)^{121}\text{I}$  reactions in the literature Acerbi et al. [1], and the impossibility to convert yield values into cross section values of that literature [2], it seems that up to 20 MeV our measurements constitute the first detailed study on the excitation function of the  $^{nat}\text{Te}(p,xn)^{121}\text{I}$  reaction.

### $^{nat}\text{Te}(p,xn)^{123}\text{I}$

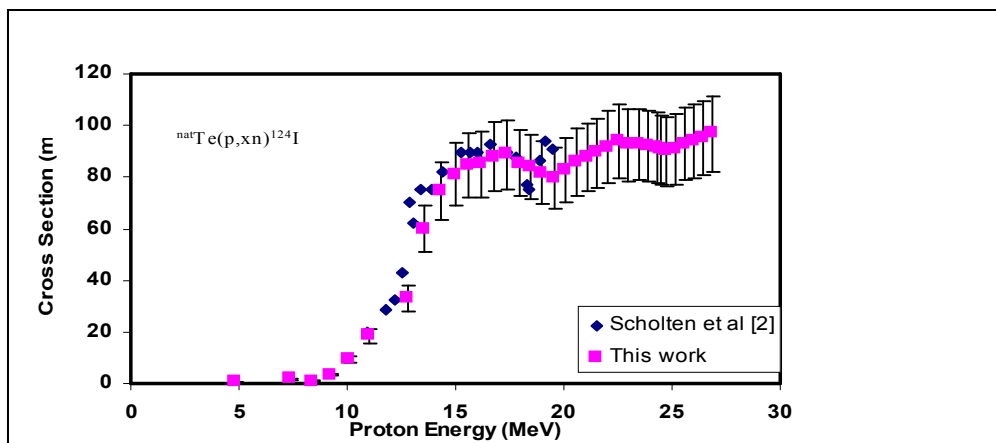
In the energy range 2-11 MeV, the reaction  $^{123}\text{Te}(p,n)^{123}\text{I}$  could be the only contributing reaction with a low maximum value of 5 mb at about 11 MeV. A broad peak around 17 MeV is due to the contribution of  $^{124}\text{Te}(p,2n)^{123}\text{I}$ . Above its 18 MeV threshold the  $^{125}\text{Te}(p,3n)^{123}\text{I}$  reaction could be responsible for the increase in the cross section value up to 160 mb at the end of the studied energy range. The present cross-section data are in good agreement with Scholten et al. [2] in Figure 2., in the limited reported energy range while no existing data for  $E_p \geq 18$  MeV had been found.

### $^{nat}\text{Te}(p,xn)^{124}\text{I}$

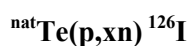
The contribution of the  $^{124}\text{Te}(p, n)$  reaction to the formation of  $^{124}\text{I}$  radionuclide, which starts at 3.9 MeV seems to be small compared with the  $^{125}\text{Te}(p, 2n)^{124}\text{I}$  and  $^{126}\text{Te}(p,3 n)^{124}\text{I}$  reactions .Figure 3. shows an acceptable agreement between present data and Scholten et al. [2] data at  $E_p \leq 18$  MeV. The  $^{125}\text{Te}(p, 2n)^{124}\text{I}$  reaction gave the first remarkable peak for the excitation function (90 mb) at  $E_p \approx 18$  MeV. Second peak can be seen at  $E_p = 23$  MeV due to the  $^{126}\text{Te}(p,3n)^{124}\text{I}$  reaction. Another increase of the cross-sections at  $E_p > 26$  MeV indicating the possible contribution of  $^{128}\text{Te}(p,5n)^{124}\text{I}$  reaction.



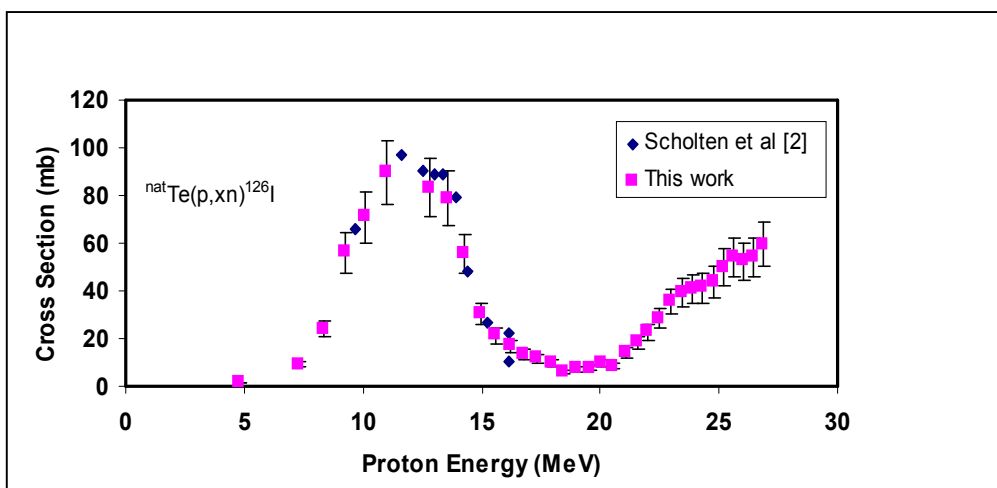
**Figure 2.** Excitation function of  $^{nat}\text{Te}(p,xn)^{123}\text{I}$  reaction along with the previously available experimental data [2].



**Figure 3.** Excitation function of  ${}^{\text{nat}}\text{Te}(p,xn){}^{124}\text{I}$  reaction along with the previously available experimental data[2].



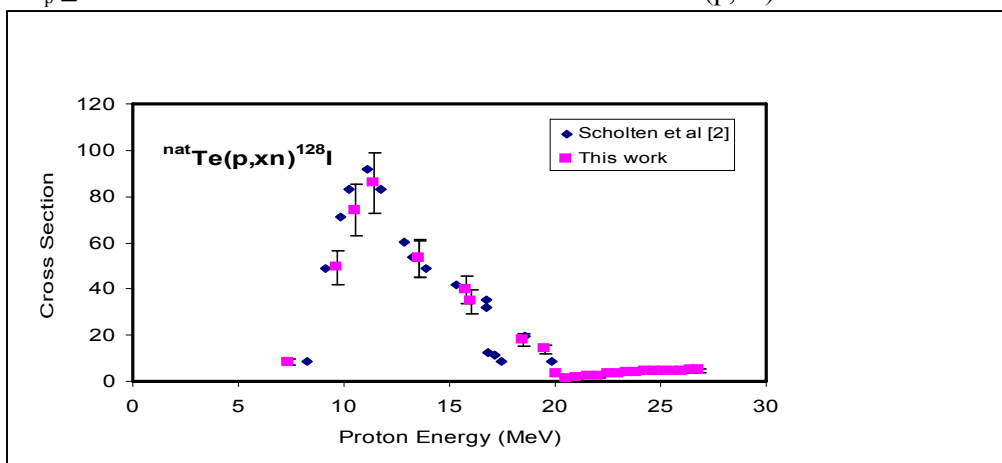
The present cross section data are in good agreement with the available reported results of Scholten et al. [2] Figure 4. At low energies a peak starts, and is due to the contribution of  ${}^{126}\text{Te}(p, n){}^{126}\text{I}$  reaction. The clear gaussian shape of the excitation function indicates the compound nucleus mechanism for this reaction. The reaction  ${}^{128}\text{Te}(p,3n){}^{126}\text{I}$  starts to construct a second peak, which could show a maximum value at less than 30 MeV.



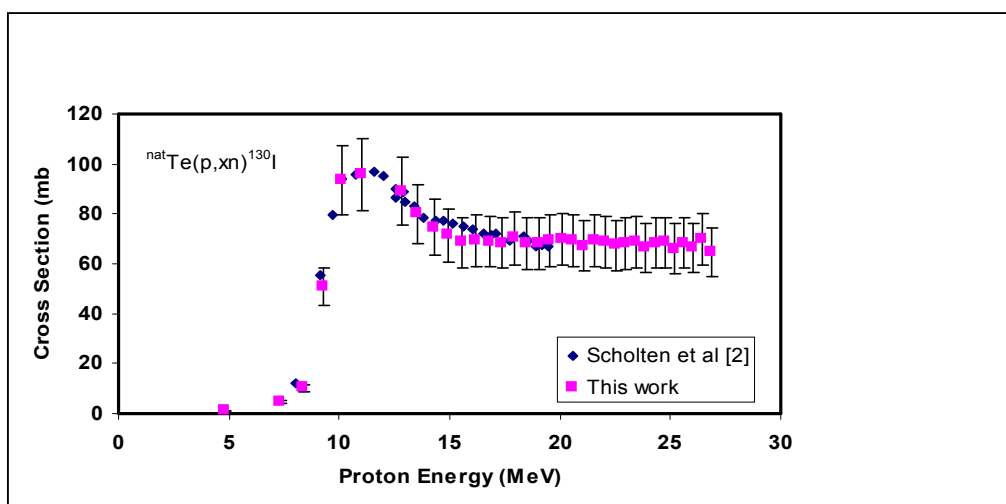
**Figure 4.** Excitation function of  ${}^{\text{nat}}\text{Te}(p,xn){}^{126}\text{I}$  reaction along with the previously available experimental data[2].

$${}^{\text{nat}}\text{Te}(p,xn){}^{128}\text{I}$$

The cross section values for  ${}^{\text{nat}}\text{Te}(p,xn){}^{128}\text{I}$  were measured for the energy range from about 2 MeV up to 27.5 MeV and the results are presented with Scholten et al. [2] data in Figure 5. The contribution of the  ${}^{128}\text{Te}(p, n){}^{128}\text{I}$  reaction is clear through the excitation function peak, 85 mb at 11.5 MeV,. An increase in the cross-section values at  $E_p \geq 20$  MeV indicates the small contribution of the  ${}^{130}\text{Te}(p,3n){}^{128}\text{I}$  reaction



**Figure 5.** Excitation function of  ${}^{\text{nat}}\text{Te}(p,xn){}^{128}\text{I}$  reaction along with the previously available experimental data[2].

$${}^{\text{nat}}\text{Te}(p,xn){}^{130}\text{I}$$


**Figure 6.** Excitation function of  ${}^{\text{nat}}\text{Te}(p,xn){}^{130}\text{I}$  reaction along with the previously available experimental data[2]

The excitation function starts at about 1.2 MeV shows that the reaction  $^{130}\text{Te}(p, n)^{130}\text{I}$  is the only contributing one. The present cross-section data are in good agreement with Scholten et al. [2]. As shown in Figure 6, the continuation of the cross section with approximately constant values after the Gaussian peak could be due to the excitation of the compound nucleus to the continuum region or some contribution of the direct reactions mechanism.

### Integral Yield

From the curves drawn through our experimental data for the  $^{\text{nat}}\text{Te}(p, xn)$  reactions, the differential and integral yields of  $^{121}\text{I}$ ,  $^{123}\text{I}$ ,  $^{124}\text{I}$ ,  $^{125}\text{I}$ ,  $^{126}\text{I}$ ,  $^{128}\text{I}$  and  $^{130}\text{I}$  were calculated, assuming an irradiation time of 1 h and a beam current of 1  $\mu\text{A}$ . The calculated integral yields are shown in Figure 7, as a function of proton energy. The yields differ considerably from one radionuclide to another, due to differences in reaction cross sections and half-lives of the products. The presented yields were compared with Scholten et al. [2] data. There was an acceptable agreement, similar to the agreement in the excitation functions.

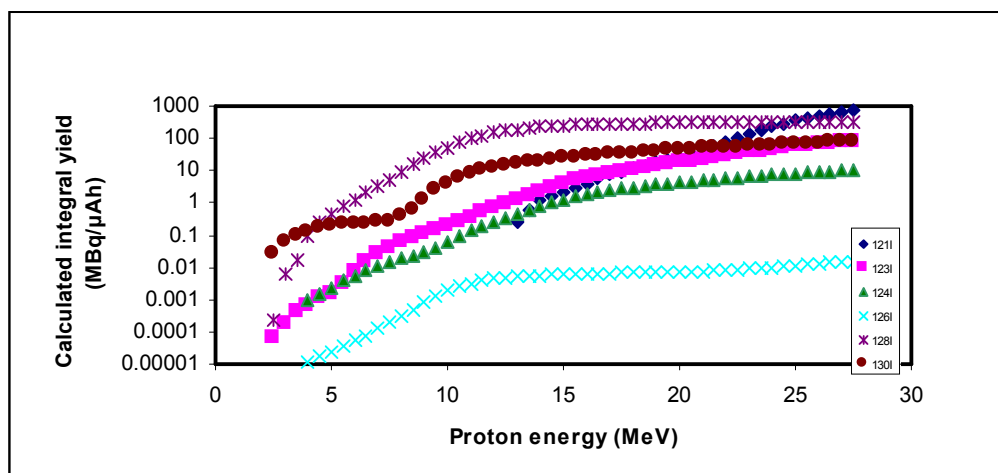


**Figure 7.** Calculated integral target yields of some radioiodines as a function of incident proton energy on natural tellurium.

### CONCLUSION

The level of the  $^{121}\text{I}$  and  $^{128}\text{I}$  impurities increases with the increasing of proton energy, this would, however, do not lead to any big problem due to their shorter half-lives in comparison with  $^{123}\text{I}$ . The level of  $^{130}\text{I}$ -impurity is fairly high, because of the high abundance of  $^{130}\text{Te}$  in the natural tellurium target material. After 6 days of EOB,  $^{124}\text{I}$  and  $^{126}\text{I}$  will be the major activities. From the above discussion enriched  $^{123}\text{Te}$  targets are essential for producing  $^{123}\text{I}$  for medical purposes.

## ACKNOWLEDGEMENTS

The authors thank Dr. Sultan Al-Sedairy (The executive Director of Research Center in king Faisal Specialist Hospital) for giving us the opportunity for target irradiation in the Research Center. The staff of Cyclotron and Radiopharmaceuticals Department especially (Eng. Salman Miliebari, Eng. Salam Rahma,, Eng. Ahmed Alghaitland Suliman Al -Yanbawi) are kindly acknowledged.

## REFERENCES

- [1] Qaim, S.M., and Stocklin, G., *Radiochim. Acta*, **34**, 25(1983).
- [2] Scholten, B., Qaim, S.M., and Stocklin, G., *Appl. Radiat. Isot.*, **40**, 127 (1989).
- [3] Ando, L., Mikecz, P.A., Tcheltsov, N.I., Suvorov, A., and Mahunka, I., *J.Radional, Nucl. Chem. Lett*, **146**,169(1990).
- [4] Stocklin, G., Qaim, S.M., and Rosch, F., *Radiochim. Acta*, **70/71**, 249-272(1995).
- [5] Tarkanyi, F., Qaim, S.M., Stocklin, G., Sajjad, M., Lambrechr, R.M., and Schweickert H, *Appl. Radiat. Isot.*, **42**, 221(1991).
- [6] Bakir, M.A., Babich, J.W., Styles, J.M, Dean, C.J., Eccies, S.A., and Lambrecht, R.M., Lambrecht, *Nuci. Med.*, **31**, 777 (1990).
- [7] Wilson, C.B., Snook, D.E., Dhokia, B., Taylor, C.V., Watson, I.A., Lammertsma, A.A., Lambrecht, R., Waxman, J., Jones T., and Epenetos A.A., *Int. J. Cancer*, **47**, 344(1991).
- [8] Scholten, B., Kovacs, Z., Tarkanyi, F., and Qaim, S.M., *Appl. Radiat. Isot.*, **46**, 255259 (1995).
- [9] Andersen, H.H., and Ziegler, J.F., in: Ziegler, J.F., (Ed.), "The Stopping and Ranges of Ions in Matter", Vol. 3, Pergamon, New York, (1977).
- [10] Gul, K., Hermanne, A., Mustafa, M.G., Nortier, F.M., Oblozinsky, P., Qaim, S.M., Scholten, B., Shubin, Yu., Takaacs, S., Tarkanyi, T.F. and Zhuang, Y., "Reference Charged Particle Cross-Section Database for Medical Radioisotope Production, Diagnostic Radio Isotopes and Monitor Reactions", IAEA-TECDOC-**1211** IAEA, Vienna, Austria, (2001).
- [11] Firestone, R.B., "Table of Isotopes, Lawrence Berkeley National laboratory", University of California, (1998).
- [12] Group T-16 (Nuclear Physics) of the Theoretical Division of the [Los Alamos National Laboratory](http://T2.Lanl.of/Data/Data.html), <http://T2.Lanl.of/Data/Data.html>, Nuclear Information Service, (1997).
- [13] Acerbi, E., Birattari, C., Castiglioni, M., and Resmini, F, *Appl. Radiat. Isot.*, **26**, 741(1975).

## دراسة دالة الإثارة للتفاعلات (p,xn) علي هدف من التيليريوم الطبيعي عند الطاقات المنخفضة للسيكلوترون: خاصة إنتاج نظير اليود-123 الطبي المشع.

خديجة زارع، نورة الحماد و أحمد عزام\*

قسم الفيزياء – كلية التربية للبنات بالرياض – الأقسام العلمية – المملكة العربية السعودية.  
\* قسم الطبيعة النووية التجريبية – مركز البحوث النووية – هيئة الطاقة الذرية – القاهرة – ج.م.ع.

تم قياس دوال الإثارة للتفاعلات النووية  $^{121,123,124,126,128,130}\text{I}$  natTe(p,xn) ، وذلك باستخدام تقانة الشرائح الملتصقة وبطاقة للبروتون تبدأ من طاقة العتبة لكل تفاعل نووي وحتى 27,5 مليون إلكترون فولت. يتم ترسيب غشاء رقيق ورفيع من natTe علي شرائح Ti بطريقة الترسيب الكهربائي. تتوافق البيانات النووية الناتجة مع القيم المنشورة – مع الأخذ في الاعتبار الخطأ المعلمي – في مدي الطاقة الأقل من 20 مليون إلكترون فولت. وعند الطاقات الأعلى من 20 مليون إلكترون فولت تم حساب قيم جديدة للمقطع المستعرض. من البيانات المقاسة للمقطع المستعرض تم حساب الناتج التكاملي للنظير  $^{123}\text{I}$  وكذلك الناتج التكاملي لشوائبة النظائرية  $^{121,124,126,128,130}\text{I}$ .